

## Helicoid to Spiral Ribbon Transition

Rouzbeh Ghafouri and Robijn Bruinsma

*Department of Physics and Astronomy, University of California, Los Angeles, California 90025, USA*  
(Received 10 September 2004; published 4 April 2005)

We present a continuum description for the transition between the helicoid and spiral ribbon structures of chiral materials. At a critical value of the ratio between the bending and stretching moduli, the Föppl–von Kármán number, we encounter a continuous buckling transition from a straight helicoid to a spiral ribbon. Two of the three persistence lengths of the ribbon become very short at the transition point, indicating strong thermal shape fluctuations. The transition is discontinuous if the ribbon width is treated as a free thermodynamic variable.

DOI: 10.1103/PhysRevLett.94.138101

PACS numbers: 87.16.Ka, 05.70.Np, 87.15.Nn, 82.35.Pq

The molecules of life, such as proteins, DNA, RNA, or the polysaccharides, are nearly all optically active due to an absence of mirror symmetry, or *chirality* [1]. Molecular chirality can be reflected in higher-level structural motifs of biomaterials that are constituted from such molecules. One familiar example is the helical organization of chitin in arthropod cuticles [2], of collagen protein in skeletal tissue [3], and of the cellulose fibrils in plant cell walls [4]. In these materials, twisted microfibrils rotate with respect to each other along a direction perpendicular to the fibril axis in the form of a *helicoid* [Fig. 1(a)]. The resulting layered “plywood” organization provides helicoidal solids with superior elastic properties, such as low Poisson ratios. Another characteristic chiral motif is the *spiral ribbon* [Fig. 1(b)]. Molecular bilayers composed of chiral lipids or other chiral surfactants can self-assemble into spiral ribbons or barber-pole tubules [5]. The helicoidal and spiral ribbon structures would appear to constitute two separate classes of chiral morphology, as is reflected in their respective descriptions. The classical continuum theory for chiral ribbons, due to Helfrich and Prost (HP) [6], is based on the assumption that the ribbon is “isometric,” i.e., that it does not support elastic strain. Chiral twist can be imposed on isometric ribbons only by winding them over the surface of a cylinder [as in Fig. 1(b)] or a cone, which is consistent with the observed spiral ribbon and tubule structures. On the other hand, if one does allow a ribbon to be stretched but now forbids any lateral bending along its axis, then the geometry of the ribbon is restricted to the family of “ruled surfaces” [7]. This family includes the helicoid, a twisted minimal surface with zero mean curvature, and other geometries such as the hyperboloid surfaces, but *not* isometric spiral ribbons. Examples of intermediate cases are, however, known, such as polypeptide  $\beta$  sheets inside folded proteins [8]. A recent Monte Carlo simulation by Selinger *et al.* [9] of chiral ribbons indeed encountered a range of structures interpolating smoothly between the helicoid and the isometric spiral ribbon with no discernible transition point.

The central role of elastic strain in this context is related to the *Theorema Egregium* of Gauss, which states that

the Gaussian curvature  $K$  of an isometric surface must remain constant under smooth bending deformations. Bending a flat ribbon with  $K = 0$  over a cylinder surface maintains isometry, but twisting it into to a helicoid surface with  $K < 0$  necessarily introduces elastic strain. It is indeed easy to see that a ribbon is elastically stretched along its edges if it is twisted up. The determination of the shape of a surface with competing in-plane elastic energy and

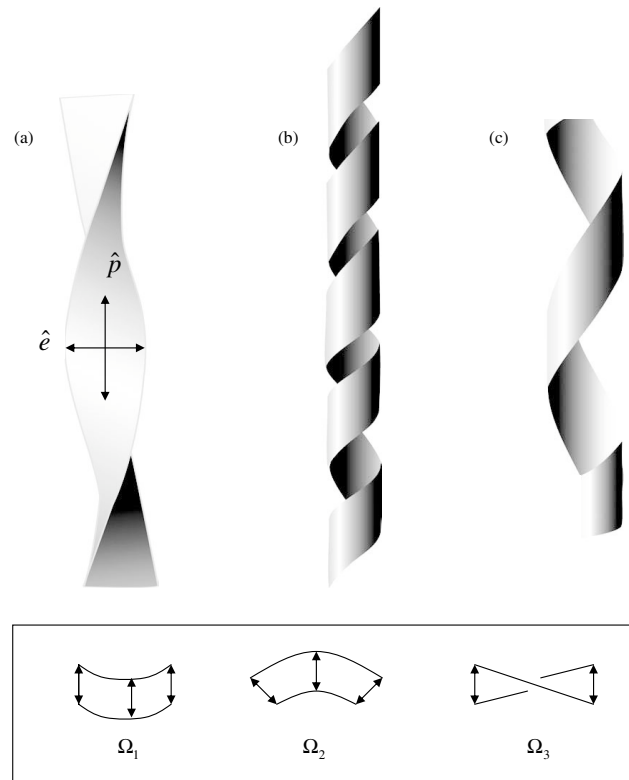


FIG. 1. Characteristic chiral ribbon configurations. (a) Helicoid with  $\Omega_1 = \Omega_2 = 0$  and  $\Omega_3$  finite. The orthogonal  $\hat{e}$  and  $\hat{p}$  directions determine the coordinate system. (b) Isometric spiral with  $\Omega_2 = 0$  and both  $\Omega_1$  and  $\Omega_3$  finite. (c) Intermediate configuration with a Föppl–von Kármán number close to its critical value. Inset: Components of the Kirchhoff rotation vector  $\vec{\Omega}$ . Only the  $\hat{e}$  direction is shown.

out-of-plane bending energy is a classical problem of elasticity theory requiring the solution of a complex set of nonlinear, coupled equations [10], due to Föppl and von Kármán (FvK), that normally do not permit analytical solution. The purpose of this Letter is to note that for chiral ribbons the FvK problem is analytically tractable and that there *is* in fact a sharp transition point between helicoids and spiral ribbons. This transition point should be characterized by strong thermal shape fluctuations.

Assume a ribbon of width  $w$  and length  $L \gg w$ . We will use an in-plane orthogonal coordinate system with the  $\hat{p}$  direction running parallel to the ribbon axis and the  $\hat{e}$  direction perpendicular to the ribbon axis [see Fig. 1(a)]. The ribbon axis is the line  $e = 0$  and the ribbon edges are at  $e = \pm w/2$ . We will assume that these  $\hat{e}$  and  $\hat{p}$  directions represent 180° rotation axes. The Hamiltonian is the sum of a bending energy  $H_b$ , an elastic energy  $H_s$ , and an energy cost  $\tau L$  for the ribbon edges:

$$H = H_b + H_s + \tau L. \quad (1)$$

Following HP, the bending energy is written as an expansion to second order in the curvature tensor  $C_{ij}$  of the ribbon, consistent with the assumed rectangular symmetry:

$$H_b = \frac{1}{2} \int d^2S (\kappa_{ee} C_{ee}^2 + \kappa_{pp} C_{pp}^2 + 2\kappa_{ep} C_{ep}^2 - 4\kappa_{ep} C_0 C_{ep} + 2\kappa_G K) \quad (2)$$

( $C_{ij} = 0$  for a flat ribbon). Here,  $\kappa_{ij}$  is the matrix of bending energy moduli. The bending energy modulus  $\kappa_{ee}$  describes, for instance, the energy cost of bending the ribbon lateral along its axis. Terms linear in  $C_{ee}$  or  $C_{pp}$  are forbidden by the assumed symmetry, but for a chiral ribbon the term  $\kappa_{ep} C_0 C_{ep}$ , which is odd under mirror reflection, is permitted. The quantity  $C_0$  plays here the role of a preferred spontaneous twist curvature. The Gaussian curvature  $K$ , in the last term of Eq. (2), is related to the curvature tensor by  $K \equiv C_{ee} C_{pp} - C_{ep}^2$  and has an associated bending modulus  $\kappa_G$ . Next, the elastic energy has the standard form  $H_s = \frac{1}{2} \int d^2S (\sigma_{ij} u_{ij})$ . The stress tensor  $\sigma_{ij}$  and the strain tensor  $u_{ij}$  are related by  $\sigma_{ij} = \lambda_{ijkl} u_{kl}$ , with  $\lambda_{ijkl}$  the matrix of elastic coefficients. For a ribbon with isotropic elastic properties, the only nonzero components are  $\lambda_{eepp} = \lambda$ ,  $\lambda_{epep} = 2\mu$ , and  $\lambda_{eeee} = \lambda_{pppp} = 2\mu + \lambda$ , with  $\mu$  and  $\lambda$  known as the Lamé coefficients. Finally, the line energy  $\tau L$ , with  $\tau$  an energy cost per unit length, describes the energy cost of the edge of the ribbon.

The coupling between in-plane elastic strain and out-of-plane bending follows from the definition of the strain tensor [10]:

$$u_{ij} = u_{ij}^* + \frac{1}{2} \frac{\partial f}{\partial x_i} \frac{\partial f}{\partial x_j}. \quad (3)$$

Here,  $u_{ij}^* = \frac{1}{2} (\partial_i u_j + \partial_j u_i)$  depends only on the in-plane displacement field  $\vec{u}(\vec{r})$  of the ribbon and  $f(\vec{r})$  is the out-

of-plane normal displacement. For a smoothly varying  $f(\vec{r})$ , the curvature tensor equals  $C_{ij} \approx \partial^2 f / \partial x_i \partial x_j$ . Using  $\sigma_{ij} = \lambda_{ijkl} u_{kl}$ , one can obtain from Eq. (3) a relation between the in-plane stress and the local Gaussian curvature  $K(\vec{r})$  [10]:

$$\frac{1}{K_0} \Delta^2 \chi(\vec{r}) = -K(\vec{r}). \quad (4)$$

Here,  $K_0 = \frac{4\mu(\mu+\lambda)}{2\mu+\lambda}$  is the 2D Young's modulus and  $\chi(\vec{r})$  is the Airy stress function [the stress tensor follows from  $\chi(\vec{r})$  by  $\sigma_{ee} = \partial^2 \chi / \partial p^2$ ,  $\sigma_{pp} = \partial^2 \chi / \partial e^2$ , and  $\sigma_{ep} = -(\partial^2 \chi / \partial e \partial p)$ ]. For a narrow ribbon, with stress-free boundary conditions, the curvature should be nearly constant along the transverse ( $\hat{e}$ ) direction, in which case the solution of Eq. (4) is straightforward. We then obtain a simple expression for the ribbon Hamiltonian with  $\kappa_g = 0$ :

$$H / (\kappa_{ee} \hat{w} C_0) \cong \frac{1}{2} \int_0^L dp \left\{ \hat{I}_1 \hat{\Omega}_1^2 + \hat{I}_2 \hat{\Omega}_2^2 + \hat{I}_3 (\hat{\Omega}_3^2 - 2\hat{\Omega}_3) + \frac{\hat{\Omega}_3^4}{320/\gamma + \hat{\Omega}_1^2} + 2\hat{\tau}/\hat{w} \right\}. \quad (5)$$

We introduced here the *Kirchhoff rotation vector*  $\vec{\Omega}(p)$  of the ribbon [10], the rate of rotation along the ribbon axis of an orthogonal coordinate system attached to the ribbon. Taking  $\hat{p}$ ,  $\hat{e}$ , and the normal to the ribbon as the orthogonal triad of unit vectors attached to the ribbon, the components of the rotation vector are  $\Omega_1(p) = C_{pp}$ , the bending curvature of the ribbon axis,  $\Omega_2(p)$  the in-plane elastic ‘‘splay’’ deformation of a ribbon, and  $\Omega_3(p) = C_{ep}$  the rotary twist of the ribbon along its axis (see Fig. 1, inset). The dimensionless rotation vector is defined as  $\hat{\Omega}_i(p) = \Omega_i(p)/C_0$ . The dimensionless prefactors of the quadratic terms of Eq. (5) are  $\hat{I}_1 = \kappa_{pp}/\kappa_{ee}$ ,  $\hat{I}_2 = \gamma \hat{w}^2/6$ , and  $\hat{I}_3 = 2\kappa_{ep}/\kappa_{ee}$ . Next,  $\gamma = K_0 \hat{w}^4 / \kappa_{ee} C_0^2$  is a dimensionless parameter and  $\hat{w} = C_0 w$  the dimensionless ribbon width. Finally,  $\hat{\tau} = \tau / \kappa_{ee} C_0$  is the dimensionless energy cost per unit length of the edges of the ribbon.

The general form of the first three terms could have been obtained by an expansion of the Hamiltonian to second order in powers of the rotation vector  $\vec{\Omega}(p)$ , excluding terms that are symmetry forbidden [11]. Together, these three terms constitute the well-known *wormlike chain* (WLC) elastic energy of a semiflexible, chiral chain, which has been very useful as a continuum theory for DNA chains. Whether the physical properties of a chiral ribbon also can be described by the WLC depends on the value of the parameter  $\gamma$ . In the limit  $\gamma \rightarrow 0$ , the fourth term of  $H$  can be neglected, and  $H$  obviously reduces to the WLC energy. Minimizing  $H$  with respect to  $\vec{\Omega}(p)$  in this regime gives  $\hat{\Omega}_i(p) = \hat{\Omega}_i^*$ , with  $\hat{\Omega}_1^* = 0$ ,  $\hat{\Omega}_2^* = 0$ , and  $\hat{\Omega}_3^* \cong 1 - \frac{\hat{\gamma}}{160\hat{I}_3}$ , which corresponds to a helicoid of pitch  $\hat{\Omega}_3^*$ , zero mean curvature, and Gaussian curvature  $K = -\Omega_3^{*2} / [1 + (w\Omega_3^*/2)^2]^2$ . In the opposite limit,  $\gamma \rightarrow \infty$ , the fourth

term is *singular*,  $\hat{\Omega}_3^4/\hat{\Omega}_1^2$ , and not of the WLC form. Minimizing  $H$  with respect to  $\hat{\Omega}(p)$  for general  $\gamma$ , gives

$$\hat{\Omega}_3^* = \frac{1}{1 + 2\sqrt{\hat{I}_1/\hat{I}_3}}, \quad \hat{\Omega}_2^* = 0, \quad (6)$$

$$\hat{\Omega}_1^*(\gamma) = \sqrt{\frac{1}{\sqrt{\hat{I}_1}} \hat{\Omega}_3^{*2} - 320/\gamma},$$

for  $\gamma > \gamma_c$  with  $\gamma_c = 320 \hat{I}_1^{1/2} (1 + 2\sqrt{\hat{I}_1/\hat{I}_3})$ . In the limit  $\gamma \rightarrow \infty$ , Eq. (6) corresponds to the isometric spiral ribbon of the HP theory. As we reduce  $\gamma$ , the twist curvature  $\hat{\Omega}_3^*$  does not change, but the bend curvature  $\hat{\Omega}_1^*(\gamma)$  of the ribbon axis vanishes continuously at  $\gamma = \gamma_c$ . For  $\gamma < \gamma_c$ ,  $\hat{\Omega}_1^*(\gamma) = 0$ , and one recovers a straight helicoid.

The parameter  $\gamma = K_0 w^4 C_0^2 / \kappa_{ee}$  evidently determines the ribbon morphology. The physical meaning of  $\gamma$  can be understood by noting that the relative area increase  $\Delta S/S$  of a ribbon twisted by an amount  $C_0$  along its axis is an even function of  $C_0$ , and of order  $(wC_0)^2$ . The elastic stretching energy per unit area of a twisted ribbon is then of the order  $K_0(wC_0)^4$ . The  $\gamma$  parameter is thus the dimensionless ratio of the stretching energy per unit area of ribbon over  $\kappa_{ee} C_0^2$ , the characteristic lateral bending energy per unit area. In the literature on elastic shells [12], such a ratio is referred to as a *FvK number*. The physical origin of the singular term  $\hat{\Omega}_3^4/\hat{\Omega}_1^2$  for  $\gamma \rightarrow \infty$  can now be understood. In the  $\gamma \rightarrow \infty$  limit, the ribbon should be isometric. Inserting the condition  $C_{ee}C_{pp} - C_{ep}^2 = 0$  in the  $C_{ee}$  curvature term of the bending energy Eq. (2) directly produces the singular term.

There is thus a sharp onset point for the helicoid/spiral ribbon transformation as a function of  $\gamma$ . The continuous growth of the bending curvature  $\hat{\Omega}_1^*(\gamma)$  for  $\gamma > \gamma_c$  is suggestive of a second-order structural phase transition, though presumably ‘‘smeared’’ by the one-dimensional nature of the problem. The elastic energy  $H$  [Eq. (5)] with  $\hat{\Omega}_i(p) = \hat{\Omega}_i^*$  indeed has a discontinuity in the second derivative at  $\gamma = \gamma_c$ . However, one encounters a surprise for the orientational correlation length, or *persistence length*, which would be expected to diverge at  $\gamma = \gamma_c$ . This persistence length can be computed from the variational energy  $\delta H$  for small fluctuations around  $\hat{\Omega} = \hat{\Omega}^*$ . For  $\gamma < \gamma_c$ ,  $\delta H$  is an asymmetric variant of the WLC energy:

$$\delta H \propto \frac{1}{2} \int_0^L dp \{ I_{1\text{eff}} \delta \hat{\Omega}_1^2 + I_{2\text{eff}}(\hat{w}) \delta \hat{\Omega}_2^2 + I_{3\text{eff}} \delta \hat{\Omega}_3^2 \}, \quad (7)$$

with  $I_{1\text{eff}} = \hat{I}_1 - (\frac{\gamma}{320})^2 \Omega_3^{*4}$ ,  $I_{2\text{eff}} = \hat{I}_2$ , and  $I_{3\text{eff}} = \hat{I}_3 + (\frac{3\gamma}{160}) \Omega_3^{*2}$ . Note that  $\hat{I}_{1\text{eff}}$  vanishes at  $\gamma = \gamma_c$ . Using a technique familiar from studies of the WLC [13], the orientational fluctuations of the ribbon around the helicoid  $\hat{\Omega}_i(p) = \hat{\Omega}_i^*$  described by Eq. (7) can be mapped onto the

quantum fluctuations of the *asymmetrical quantum top* [14]:

$$\delta \hat{H} \propto \frac{1}{2} \left( \frac{\hat{L}_1^2}{I_{1\text{eff}}} + \frac{\hat{L}_2^2}{I_{2\text{eff}}} + \frac{\hat{L}_3^2}{I_{3\text{eff}}} \right), \quad (8)$$

with  $\hat{L}$  the angular momentum operator. The three  $J = 1$  eigenstates of  $\delta \hat{H}$  correspond to three separate orientational persistence lengths:

$$1/\xi_1 = \frac{k_B T}{2\kappa_{ee} w} \left( \frac{1}{I_{2\text{eff}}} + \frac{1}{I_{3\text{eff}}} \right);$$

$$1/\xi_2 = \frac{k_B T}{2\kappa_{ee} w} \left( \frac{1}{I_{3\text{eff}}} + \frac{1}{I_{1\text{eff}}} \right); \quad (9)$$

$$1/\xi_3 = \frac{k_B T}{2\kappa_{ee} w} \left( \frac{1}{I_{1\text{eff}}} + \frac{1}{I_{2\text{eff}}} \right).$$

$\xi_3$  is the persistence length of the tangent to the ribbon axis,  $\xi_2$  the persistence length of the normal to the ribbon surface, and  $\xi_1$  the persistence length of  $\hat{e}$ , the remaining orthogonal direction. Since  $I_{1\text{eff}}$  vanishes at  $\gamma = \gamma_c$ , both the  $\xi_3$  and  $\xi_2$  persistence lengths formally *vanish* at  $\gamma = \gamma_c$ . Physically, this means that near  $\gamma = \gamma_c$  the ribbon should be extremely flexible and subject to strong thermal fluctuations in its orientation.

An interesting physical consequence of the helicoid to spiral ribbon quasitransition is connected with the fact that  $\gamma$  depends on the ribbon width as  $w^4$ . A plot of  $E(w)$ , the energy minimum at  $\hat{\Omega} = \hat{\Omega}^*$ , shows two extrema as a function of increasing ribbon width (see Fig. 2), separated

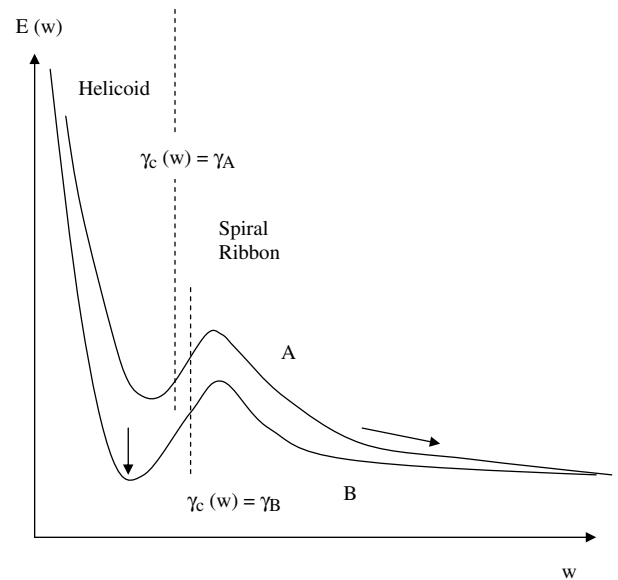


FIG. 2. Ribbon energy minimum  $E(w)$  as a function of the ribbon width  $w$  (schematic). The curve marked  $A$  corresponds to a larger value of the Föppl–von Kármán number  $\gamma$  and  $B$  to a lower value. As a function of  $\gamma$ , a first-order transition takes place from a spiral ribbon state with a large width, case  $A$ , to a helicoid state with a well-defined smaller width, case  $B$ .

by a singularity at  $\gamma = \gamma_c$ . There is first a minimum at  $\hat{w}^* = (160\hat{\tau}/\gamma \hat{\Omega}_3^{*4})^{1/5}$ , with  $\gamma(w^*) < \gamma_c$  in the helicoidal regime, followed by a maximum at  $\hat{w}^\dagger$  for  $\gamma(\hat{w}^\dagger) > \gamma_c$  in the spiral ribbon regime. Asymptotically,  $E(w \rightarrow \infty) = 0$ . If the ribbon width is viewed as a free thermodynamic variable that is to be determined by free energy minimization, then, as is clear from Fig. 2, there are just two stable states: a helicoidal ribbon of finite width  $w^*$  and an isometric spiral ribbon with  $w \rightarrow \infty$  (the barber-pole tubule in actuality): *Spiral ribbons of finite width are unstable*. If  $w$  is a free variable, then, as a function of the ratio  $K_0 C_0^2 / \kappa_{ee}$ , we should expect to encounter a *discontinuous* transition from a helicoid to a spiral tubule.

A direct numerical test of the proposed transition would be to compute the bending stiffness of the helical ribbons obtained in the low-temperature Monte Carlo simulations of Selinger *et al.* [9] and check whether their bending stiffness vanishes at  $\gamma(w) = \gamma_c$ . If the existence of the transition indeed is confirmed, then it would be very interesting to repeat the simulations at higher temperatures in order to study the conformational fluctuations that are predicted to be pronounced near  $\gamma(w) = \gamma_c$ . Important consequences of this transition for the case of  $\beta$  amyloid fibers will be presented elsewhere.

R. B. would like to thank the Newton Institute for its kind hospitality. He benefited there from discussions with C. Dobson, M. Fisher, J. Harden, T. C. B. McLeish, and R. Sears.

- [1] For a review, see A. Harris, R. Kamien, and T. C. Lubensky, *Rev. Mod. Phys.* **71**, 1745 (1999).
- [2] J. F. Revol and R. H. Marchessault, *Int. J. Biol. Macromol.* **15**, 329 (1993).
- [3] A. Bigi, L. Dovigo, M. Koch, M. Morocutti, A. Ripamonti, and N. Roveri, *Connect Tissue Res.* **25**, 171 (1991).
- [4] A. Emons and B. Mulder, *Proc. Natl. Acad. Sci. U.S.A.* **95**, 7215 (1998).
- [5] S. Pakhomov, R. P. Hammer, B. K. Mishra, and B. N. Thomas, *Proc. Natl. Acad. Sci. U.S.A.* **100**, 3040 (2003).
- [6] W. Helfrich and J. Prost, *Phys. Rev. A* **38**, 3065 (1988).
- [7] A. Gray, in *Modern Differential Geometry of Curves and Surfaces with Mathematica* (CRC Press, Boca Raton, 1993), 2nd ed., Chap. 19.
- [8] F. R. Salemme, *Prog. Biophys. Molec. Biol.* **42**, 95 (1983).
- [9] R. Selinger, J. Selinger, A. Malanoski, and J. Schnur, *Phys. Rev. Lett.* **93**, 158103 (2004).
- [10] L. D. Landau and E. M. Lifshitz, *Theory of Elasticity* (Pergamon Press, Oxford, 1976), 2nd ed., Chap. 14.
- [11] J. Marko and E. Siggia, *Macromolecules* **27**, 981 (1994).
- [12] J. Lidmar, L. Mirny, and D. R. Nelson, *Phys. Rev. E* **68**, 051910 (2003).
- [13] J. D. Moroz and P. Nelson, *Proc. Natl. Acad. Sci. U.S.A.* **94**, 14 418 (1997).
- [14] L. D. Landau and E. M. Lifshitz, *Quantum Mechanics, Non-Relativistic Theory* (Butterworth-Heinemann, Oxford, 2003), 3rd ed., Chap. 103.